Gas-Phase DNA: Oligothymidine Ion Conformers

Cherokee S. Hoaglund, Yansheng Liu, Andrew D. Ellington, Marty Pagel, and David E. Clemmer*

Department of Chemistry, Indiana University
Bloomington, Indiana 47405

Received March 3, 1997

Interest in producing gas-phase nucleic acid ions[1a−g] has been stimulated by recent mass spectrometry (MS) based sequencing strategies for biomolecules.[2a−h] Recently mass spectra for plasmid and linear DNAs having molecular weights of 10^6−10^8 daltons have been recorded.[3a−c] In contrast to the wealth of structural data for nucleic acids in solution, there is no information about conformations of the gas-phase ions. The conformations of protein ions can influence fragment formation;[4] thus, the issue of conformation is important for sequencing nucleic acids by MS. Here, we report the first study of the conformations of a deprotonated DNA oligomer in the gas phase: oligothymidine comprised of ten thymine nucleotides. Using electrospray ionization[5] and ion mobility techniques,[6] we have measured collision cross sections for the −2 to −6 states, $(T_{10}\text{-}n\text{H})^{n-}$, where n is the deprotonation state, and deprotonated states of oligothymidine with sodium ions attached $(NaT_{10}\text{-}n\text{H})^{(n-1)-}$, where $n = 5-7$. A sharp structural transition is observed when four or more protons are removed; lower charge states favor compact globular conformers and higher ones favor elongated forms. Addition of a single sodium ion to deprotonated states stabilizes more compact conformers. Conformations that were derived using molecular modeling techniques provide complementary information that allows many important structural features to be delineated.

Our experimental apparatus and procedures have been described previously.[6] Negatively-charged (deprotonated) oligothymidine ions were formed by electrospraying a $\sim 3 \times 10^{-5}$ M oligothymidine[7] solution in 49.9:49.9:0.2 water:acetonitrile: ammonium hydroxide. Sodium adducts are readily formed, although no sodium was added. Ions were extracted into a high-vacuum region and 30 microsecond pulses were injected into a drift tube containing ~3.0 Torr of helium in order to record ion mobility distributions. The drift times depend on the ions' conformations; compact conformers drift through faster than extended forms. Ions that exit the drift tube are focussed into a quadrupole mass spectrometer that transmits only the ion of interest. As ions enter the drift tube they are heated by collisions with the buffer gas. Further collisions cool the ions to the buffer gas temperature. Ion mobility distributions at varying injection energies (~150−450 eV) yield identical drift times; thus, we expect these data correspond to relatively stable conformations. Figure 1 shows charge normalized ion mobility distributions for the −2 to −6 charge states of $(T_{10}\text{-}n\text{H})^{n-}$. Each distribution shows a single peak. The −2 and −3 states have similar normalized drift times, ~5.2 ms, suggesting similar conformations. A shift to 6.2 ms is observed for the −4 charge state. The −5 and −6 ions have drift times of 7.2 and 7.4 ms, respectively. These ions favor more open conformations. Ion mobility distributions for oligothymidine ions containing sodium, $(NaT_{10}\text{-}5H)^{4-}$, $(NaT_{10}\text{-}6H)^{5-}$, and $(NaT_{10}\text{-}7H)^{6-}$, are also shown in Figure 1. The average drift time of $(NaT_{10}\text{-}7H)^{6-}$ is similar to that for $(T_{10}\text{-}6H)^{6-}$. The $(NaT_{10}\text{-}5H)^{4-}$ and $(NaT_{10}\text{-}6H)^{5-}$ ions have higher mobilities than the pure DNA ions of the same charge. Binding sodium leads to more compact conformations of these high charge states.

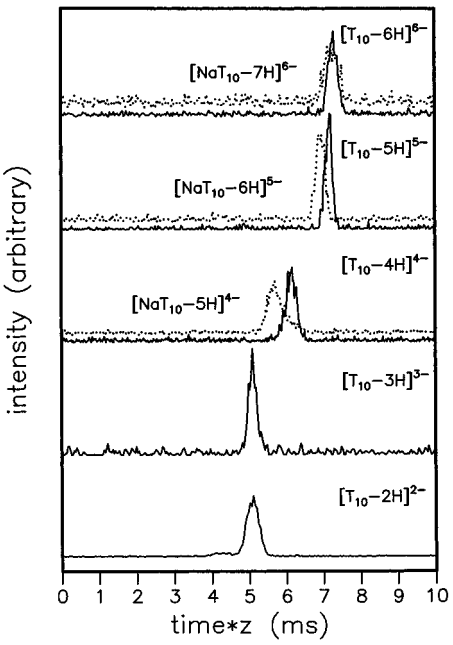

Figure 1. Ion mobility distributions for deprotonated $(T_{10}\text{-}n\text{H})^{n-}$ (solid lines) and $(NaT_{10}\text{-}n\text{H})^{(n-1)-}$ (dotted lines) ions formed by electrospray ionization. The distributions are shown on a modified time scale t*z which normalizes for differences in effective drift fields.

Drift times can be converted into experimental collision cross sections as described previously[6] and are shown in Figure 2. Additional insight was gained by comparing calculated cross sections for an array of conformers generated by molecular modeling techniques to the experimental data.[8] Trial conformers were obtained using the Insight II molecular modeling software with the CVFF forcefield.[9] The forcefield used a dielectric constant of 1.0 for the surrounding media; thus, these are *in vacuo* conformations. For each charge state, 100 different trial conformers were generated by simulated annealing. The temperature was increased to 1000 K over 2 ps, equilibrated for 2 ps, and then cooled over 1 ps to 300 K. The structures obtained were energy minimized, and the atomic coordinates of conformations that fell within 30 kcal/mol of the lowest energy model conformer were used to calculate average cross

(1) (a) Hunt, D. F.; Hignite, C. E.; Biemann, K. *Biochem. Biophys. Res. Commun.* **1968**, *33*, 378. (b) McNeal, C. J.; Ogilvie, K. K.; Theriault, N. Y.; Nemer, M. J. *J. Am. Chem. Soc.* **1982**, *104*, 976. (c) Grotjahn, L.; Frank, R.; Blocker, H. *Nucleic Acids Res.* **1982**, *10*, 4671. (d) Cerney, R. L.; Gross M. L.; Grotjahn, L. C. *Anal. Biochem.* **1986**, *156*, 424. (e) Covey, T. R.; Bonner, R. F.; Shushan, B. I.; Henion, J. D. *Rapid Commun. Mass Spectrom.* **1988**, *2*, 249. (f) Hillenkamp, F.; Karas, M.; Ingendoh, A.; Stahal, B. In *Biological Mass Spectrometry*; Burlingame, A. L., McCloskey, J. A., Eds.; Elsevier: Amsterdam, 1990. (g) Spengler, B.; Pan, Y.; Cotter, R. *Rapid Commun. Mass Spectrom.* **1990**, *4*, 99.

(2) (a) Crain, P. F. *Mass Spectrom. Rev.* **1990**, *9*, 505. (b) McLuckey, S. A.; Van Berkel, G. J.; Glish, G. L. *J. Am. Soc. Mass Spectrom.* **1992**, *3*, 60. (c) McLuckey, S. A.; Habibi-Goudzrzi, S. *J. Am. Chem. Soc.* **1993** *115*, 12085. (d) Little, D. P.; Speir, J. P.; Senko, M. W.; O'Connor, P. B.; McLafferty, F. W. *Anal. Chem.* **1994**, *66*, 2809. (e) Little, D. P.; Chorush, R. A.; Speir, J. P.; Senko, M. W.; Kelleher, N. L.; McLafferty, F. W. *J. Am. Chem. Soc.* **1994**, *116*, 4893. (f) Little, D. P.; McLafferty, F. W. *J. Am. Chem. Soc.* **1995**, *117*, 6783. (g) Christian, N. P.; Colby, S. M.; Giver, L.; Houston, C. T.; Arnold, R. J.; Ellington, A. D.; Reilly, J. P. *Rapid Commun. Mass Spectrom.* **1995**, *9*, 1061. (h) Ni, J.; Pomerantz, S. C.; Rozenski, J.; Zhang, Y.; McCloskey, J. A. *Anal. Chem.* **1996**, *68*, 1989.

(3) (a) Fuerstenau, S. D.; Benner, W. H. *Rapid Commun. Mass Spectrom.* **1995**, *9*, 1528. (b) Chen, R.; Cheng, X.; Mitchell, D. W.; Hofstadler, S. A.; Wu, Q.; Rockwood, A. S.; Sherman, M. G.; Smith, R. D. *Anal. Chem.* **1995**, *67*, 1159. (c) Cheng, X.; Camp II, D. G.; Wu, Q.; Bakhtiarl, R.; Springer, D. L.; Morris, B. J.; Bruce, J. E.; Anderson, G. A.; Edmonds, C. G.; Smith, R. D. *Nucleic Acids Res.* **1996**, *24*, 2183.

(4) Loo, J. A.; Edmonds, C. G.; Smith, R. D. *Science* **1990**, *248*, 201.

(5) Fenn, J. B.; Mann, M.; Meng, C. K.; Wong, S. F.; Whitehous, C. M. *Science* **1989**, *246*, 64.

(6) For a recent review, see: Clemmer, D. E.; Jarrold, M. F. *J. Mass. Spectrom.* **1997**, *32*, 577 and references therein.

(7) Oligothymidine used was synthesized using an Applied Biosystems 391 DNA synthesizer utilizing the phosphoramidite method. The ions studied here are dephosphorylated at the 5′ end.

(8) This approach is similar to a method discussed by Wyttenbach, T.; von Helden, G.; Bowers, M. T. *J. Am. Chem. Soc.* **1996**, *118*, 8355.

(9) Insight II; BIOSYM/MSI: San Diego, CA, 1995.

S0002-7863(97)00652-5 CCC: $14.00

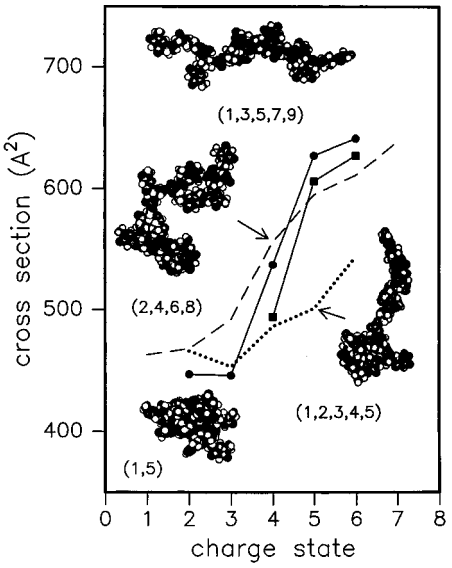

Figure 2. Experimental cross sections for the −2 to −6 states of $(T_{10}$-$nH)^{n-}$ (●) and −4 to −6 charge states of $(NaT_{10}$-$nH)^{(n-1)-}$ (■). The dotted line shows calculated cross sections for trial conformers with charges on adjacent phophodiester linkages [averages of the data denoted with asterisks (*) in Table 1]. The dashed line shows the calculated cross sections that are obtained when the deprotonation sites are distributed more evenly along T_{10}. Values plotted for evenly distributed sites correspond to averages of the data denoted with solid squares (■) in Table 1. Example model conformations are shown for the −2 (1,5), −4 (2,4,6,8), −5 (1,2,3,4,5), and −5 (1,3,5,7,9) states.

sections.[10] Cross sections are estimated by calculating the average projection when the coordinates are rotated through all possible orientations.[11]

The calculations show that the gas-phase conformation depends strongly on the number and locations of charged sites. Deprotonation should occur along the nine phosphodiester linkages; the number of possible combinations of assigning charges to sites is $9!/[n!(9-n)!]$. A summary of calculated collision cross sections for several different site assignments is given in Table 1. The effect of varying the position of charges can be seen by considering the −5 state. When charges are assigned at the 1,3,5,7,9 sites, the resulting structures have an average collision cross section of 608 ± 21 Å^2, near the experimental value (627 ± 6 Å^2). Assignment of charges to the 1,2,3,4,5 adjacent sites results in conformers with a much smaller cross section (501 ± 19 Å^2). Although there is some question about the absolute accuracy of methods for calculating cross sections,[11] relative changes in calculated values for different charge states allow us to derive probable charge site assignments. Experimental cross sections for the −4, −5, and −6 states are factors of 1.20, 1.40, and 1.43 times larger than the compact −2 and −3 states. Calculated cross sections for the −4, −5, and −6 states (with charges assigned to adjacent sites) are larger than the −2 result by factors of only ∼1.04, 1.08, and 1.17, respectively (far below the experimental increases). When charges are distributed more evenly (i.e., 1,3,5,7, 1,3,6,9, and 2,4,6,8 for the −4 state; the 1,2,5,6,9 and 1,3,5,7,9 for the −5 state; and 1,2,4,5,7,8,9 and 1,2,3,4,7,8,9 for the −6 state), the calculated cross sections are larger by factors of ∼1.19, 1.27, and 1.31. These results suggest that for the −4 to −6 states charges are distributed rather evenly along T_{10}.

Table 1. Experimental and Calculated Data for $(T_{10}$-$nH)^{n-}$ Ions

charge state	charged site[a] assignment		σ_{exp}[b] (Å^2)	σ_{proj}[c] (Å^2)
−1	2	■		453(16)
−1	4	■		468(15)
−1	6	■		455(23)
−2	1,2	*	447(5)	466(20)
−2	1,5	■		490(21)
−2	1,9	■		463(20)
−2	3,6	■		452(24)
−3	1,2,3	*	446(5)	453(19)
−3	1,3,5	■		460(23)
−3	1,5,9	■		543(30)
−3	4,5,6	*		472(19)
−4	1,2,3,4	*	537(5)	486(18)
−4	1,3,5,7	■		543(24)
−4	1,3,6,9	■		578(24)
−4	2,4,6,8	■		546(25)
−5	1,2,3,4,5	*	627(6)	501(19)
−5	1,2,5,6,9	■		581(28)
−5	1,3,5,7,9	■		608(21)
−6	1,2,3,4,5,6	*	641(6)	544(16)
−6	1,2,4,6,8,9	■		595(36)
−6	1,3,5,7,8,9	■		627(23)
−7	1,2,4,5,7,8,9	■		642(22)
−7	1,2,3,4,7,8,9	■		634(22)

[a] Charge site assignment denotes the phosphate between the first two residues on the 5′ end as site 1. [b] Experimental cross sections derived from ion mobility data. [c] Calculated cross sections for conformers generated by molecular modeling. Uncertainties are in parentheses.

The transition to more open conformers is driven by an increase in coulomb repulsion energy for high charge states; this disrupts hydrogen-bonding and van der Waals interactions that favor more compact structures. Examination of the model structures where charges are dispersed evenly or placed adjacently on T_{10} provides insight about the interactions that define the *in vacuo* conformations. When charges reside at adjacent sites, the conformer is essentially linear over the deprotonated region and globular over the remaining portion. An example is displayed for −5 (1,2,3,4,5). The linear section results from large coulombic energies in the region of neighboring charges. Globular portions of these conformers typically contain several base stacking interactions and hydrogen bonds. When charges are distributed more evenly throughout the oligomer, such as −5 (1,3,5,7,9) also shown the conformation opens up with relative uniformity. The importance of electrostatic interactions is consistent with the differences in cross sections near the structural transition region observed for $(T_{10}$-$4H)^{4-}$ and $(NaT_{10}$-$5H)^{4-}$. Although Na^+ is physically larger than a proton, the cross sections for $(NaT_{10}$-$5H)^{4-}$, $(NaT_{10}$-$6H)^{5-}$, and $(NaT_{10}$-$7H)^{6-}$, are smaller than the corresponding charge states for deprotonated T_{10}. The localized positive charge on the Na^+ leads to more compact conformations.

The conformations of nucleic acids in solution are governed by a combination of hydrophobic interactions and hydrogen bonds (attractive folding forces) and repulsive electrostatic forces. When denatured nucleic acids undergo a cooperative unfolding transition. In the gas phase, compact conformations are also held together by hydrogen bonds and van der Waals forces and are similarly disrupted by electrostatic interactions. In the absence of solvent and counterions the multiple charges repel one another causing the gas-phase nucleic acid to unfold. The unfolding transition occurs when coulomb repulsion exceeds the hydrogen bonding and van der Waals interactions between residues. Here, this transition occurs when ∼50% of the phosphodiester linkages are charged.

Acknowledgment. We thank Alex Shvartsburg and Prof. Martin Jarrold (Northwestern) for providing the EHSS code. This work was supported by the NSF (CHE-9625199).

JA970652W

(10) Diagnostic calculations showed that this annealing and minimization protocol provides a representative distribution of lowest energy structures.

(11) The accuracy of methods for calculating cross sections for very large molecules is currently being scrutinized (See ref 6). Shvartsburg and Jarrold have developed an exact hard sphere scattering (EHSS) model that rigorously accounts for scattering of buffer gas atoms: Shvartsburg, A. A.; Jarrold, M. F. *Chem. Phys. Lett.* **1996** *261*, 86. These values are viewed as upper limits to the true cross sections. For T_{10} we have calculated EHSS cross sections for a limited number of different conformer types and find that they are generally larger than projection values by ∼8−16%, for conformers that range from elongated to compact, respectively. We expect that the projection method for conformers of T_{10} (which are smaller than protein conformers) gives values that are accurate to a level that is near the uncertainties reported for the average of the many conformations that were found.